Lawrence Berkeley National Laboratory
LBL Publications

Title
Acid Site Design for Low Hydration Proton Exchange Membranes

Permalink
https://escholarship.org/uc/item/00h0f0gb

Journal
Advanced Functional Materials, 36(69)

ISSN
1616-301X

Authors
Kumar, Ajay
Alzate-Vargas, Lorena
Rodriguez-Pena, Mayra
et al.

Publication Date
2026-08-01

DOI
10.1002/adfm.77447

Copyright Information
This work is made available under the terms of a Creative Commons Attribution License, available at https://creativecommons.org/licenses/by/4.0/

Peer reviewed

eScholarship.org Powered by the California Digital Library
University of California

Check for updates

Advanced Functional Materials

ADVANCED FUNCTIONAL MATERIALS
www.afm-journal.de

RESEARCH ARTICLE OPEN ACCESS

Acid Site Design for Low Hydration Proton Exchange Membranes

Ajay Kumar[1] | Lorena Alzate-Vargas[2] | Mayra Rodriguez-Pena[1] | Douglas I. Kushner[3] | Marina Pacheco[1] | Panagiotis Bexis[1] | Ahmet Kusoglu[3] | Siddharth Komini Babu[1] | Edward F. Holby[2] | Jacob S. Spendelow[1] | Eun Joo S. Park[1]

[1]Materials Synthesis and Integrated Devices, Los Alamos National Laboratory, Los Alamos, New Mexico, USA | [2]Theoretical Division, Los Alamos National Laboratory, Los Alamos, New Mexico, USA | [3]Energy Technologies Area, Lawrence Berkeley National Laboratory, Berkeley, California, USA

Correspondence: Eun Joo S. Park (epark@lanl.gov)

Received: 12 June 2026 | **Revised:** 14 July 2026 | **Accepted:** 17 July 2026

Keywords: acid group engineering | hydration number | intrinsic acidity | polymer electrolytes | proton exchange membranes | proton transport

ABSTRACT

Hydrocarbon proton exchange membranes (PEMs) are promising PFSA-free candidates for proton exchange membrane-based electrochemical devices, but high conductivity is typically accompanied by excessive hydration and swelling. Here we introduce, for the first time in a polymer electrolyte membrane, a sulfonic acid group bearing a difluoromethylene (—CF_2—) substituent directly adjacent to the acid site. Density functional theory calculations indicate that α-CF_2 substitution effectively lowers the pK_a of alkylsulfonic acid, suggesting enhanced proton dissociation under reduced hydration. Guided by this concept, we synthesized the hydrocarbon membrane TPCF2SA and compared it with the alkylsulfonic acid analogue TPSA. TPCF2SA exhibits much lower water uptake (20 vs. 51% at 80°C), lower hydration number (λ = 6.2 vs. 15), and lower swelling, while maintaining high proton conductivity (87 vs. 79 mS cm^{-1}). Morphology analysis reveals a more distinct hydrated nanostructure for TPCF2SA at 80°C, consistent with efficient proton-transport pathways at reduced water content. In water electrolyzers, TPCF2SA delivers 3.0 A cm^{-2} at 1.79 V, strongly outperforming TPSA and approaching NR212. These results highlight acid-group design as a powerful strategy for low-hydration, high-performance hydrocarbon PEMs.

1 | Introduction

Proton exchange membranes (PEMs) are fundamental to electrochemical technologies, including fuel cells, water electrolyzers, and unitized reversible fuel cells, as they facilitate proton transport while serving as gas barriers. The functionality of a PEM depends on its proton conductive groups, specifically strong Brønsted acid sites that dissociate into mobile protons and immobile anions tethered to the polymer backbone. The efficiency of proton transport is fundamentally dictated by the intrinsic acid strength (pK_a), the density of acid sites, and the microenvironment surrounding the acid sites [1]. These variables define proton dissociation, coordination that forms a continuous hydrogen-bond network, and the activation barriers governing both Grotthuss and vehicle transport. Consequently, precise engineering of proton-donor chemistry provides the primary strategy for maximizing conductivity while balancing the competing physical constraints of water uptake, swelling, and long-term mechanical durability in the membrane.

The leading commercial PEMs are perfluorosulfonic acid (PFSA) polymers such as Nafion, valued for their high conductivity, dimensional stability, and chemical and mechanical robustness [2, 3]. Their phase-separated morphology, arising from highly acidic perfluorosulfonic acid side chains and a hydrophobic perfluorinated backbone, delivers high proton conductivity

This is an open access article under the terms of the Creative Commons Attribution-NonCommercial-NoDerivs License, which permits use and distribution in any medium, provided the original work is properly cited, the use is non-commercial and no modifications or adaptations are made.
© 2026 The Author(s). *Advanced Functional Materials* published by Wiley-VCH GmbH

(>100 mS cm^{-1}) even at relatively low ion exchange capacity (IEC, e.g., ~0.9 mequiv. g^{-1} for NR212), enabling reliable and durable operation in a wide range of devices. Although cost initially motivated the search for alternatives, growing public and regulatory attention to per- and polyfluoroalkyl substances (PFAS) [4] are now providing a clear environmental drive for developing hydrocarbon-based, low-fluorine membranes.

Many hydrocarbon membranes employ aromatic or alkyl sulfonic acids as their proton-donating group, which can be introduced by well-established chemistries: (a) post-sulfonation of the polymer using reagents such as fuming sulfuric acid (oleum), chlorosulfonic acid, trimethylsilyl chlorosulfonate, or acetyl sulfate; [5–8] (b) direct polymerization using sulfonated monomers; [9–11] and (c) functionalization with thiol precursors followed by thiol oxidation [12, 13]. The most advanced sulfonated hydrocarbon membranes have demonstrated conductivity and cell performance on par with PFSA in electrochemical devices, [14–16] although several recurring challenges still remain. Because organic sulfonic acids are generally less acidic than the perfluoroalkylsulfonic acid group in PFSA, hydrocarbon membranes typically require a higher degree of sulfonation (i.e., higher IEC) to achieve comparable proton dissociation and form a continuous hydrated conduction network [1]. Most high performing hydrocarbon PEMs with >100 mS cm^{-1} proton conductivity (at 80°C, >95% relative humidity, RH) often have IEC of >2.5 mequiv. g^{-1} [17]. Increasing the degree of sulfonation results in a trade-off between conductivity gains and membrane robustness because increased water uptake drives swelling and softening, increasing the risk of mechanical failure of membranes. High water uptake and swelling also facilitate radical access and attack, [18] accelerating chemical and mechanical degradation. In addition, conductivity drops sharply at low RH and elevated temperature as water content decreases and the activation barrier for proton transport increases. This performance profile does not align with modern fuel-cell targets, which favor lower RH, higher temperature operation for faster reaction kinetics and simplified water management [19]. In water electrolyzers, where membranes operate under highly hydrated conditions, excessive water uptake and dimensional swelling can compromise mechanical integrity, increase gas crossover, and reduce long-term durability under continuous operation. Therefore, membrane design requires a careful balance between maintaining high proton conductivity and limiting excessive water uptake and swelling to ensure stable performance across both low-humidity fuel cell and fully hydrated electrolyzer operating conditions. Strategies such as reinforcement, crosslinking, or other forms of mechanical enhancement are therefore necessary for practical implementation of hydrocarbon membranes [15, 20].

In this work, we focus on engineering the acid site to tune Brønsted acidity of sulfonic acid, creating stronger and more accessible proton conducting sites while limiting excessive swelling in hydrocarbon PEMs. Our approach introduces a previously unreported organic sulfonic acid motif within a hydrocarbon polymer architecture: an alkylsulfonic acid group bearing a difluoromethylene (—CF_2—) substituent directly adjacent (α) to the acid site. While related OCF_2SO_3H-containing hydrocarbon PEMs have been reported [21], the present α-CF_2 alkyl sulfonic acid structure is distinct and, to our knowledge, has not previously been incorporated into hydrocarbon PEMs. This strategy does not rely on perfluoroalkyl chains, yet it still delivers enhanced acidity relative to simple alkylsulfonic acids. The α-CF_2 group acts as a localized electron-withdrawing substituent that stabilizes the sulfonate conjugate base and lowers the energy barrier for proton dissociation and transport. This study demonstrates that targeted redesign of the acid functionality can enhance proton transport performance in hydrocarbon membranes while reducing reliance on high membrane hydration.

2 | Results and Discussion

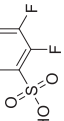
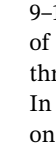
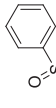
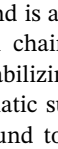
2.1 | pK_a Value Calculation for Strong Sulfonic Acids

Measuring experimental pK_a values for very strong sulfonic acids ($pK_a < -2$) is inherently challenging [22]. In water, these acids are often fully dissociated, and the definition of their pK_a values becomes sensitive to activity coefficients, ion pairing, and the choice of reference state and measurement method [23], rather than being accessible by straightforward titration. To enable a comparable measure of strong acid compounds, we evaluated acidity by calculating aqueous pK_a values for organic sulfonic acid compounds and their fluorinated counterparts under the same computational model and solvation assumptions using density functional theory (DFT) calculations. This approach has proven reliable for assessing relative trends [24, 25], allowing comparison of the Brønsted acidity of these sulfonic acids on a common scale, even when absolute experimental pK_a values are difficult to obtain or unavailable in the literature.

Two pK_a calculation schemes were employed: an empirical cycle (Cycle A) [26] and a thermodynamic cycle (Cycle B) [27]. These methods differ in their treatment of proton solvation: Cycle A relies on the experimental absolute solvation free energy of the proton, whereas Cycle B instead uses the hydronium–water pair as a reference, thereby avoiding direct treatment of the proton in solution. A detailed description of both schemes is provided in the Supporting Information. For each scheme, both gas-phase and solvated structures were optimized at two different levels of theory: the hybrid B3LYP and the hybrid meta-GGA M06-2X, to account for the electron exchange and correlation contribution to systems' Hamiltonian. The same basis set, 6–311++G(2d,2p), was employed for all calculations. Solvation effects were treated using an implicit continuum model (SMD) to represent the aqueous environment. All computed pK_a values, including results from both thermodynamic cycles and both levels of theory, are summarized in Table 1. We validated these approaches using benchmark acids with reported experimental pK_a values: methanesulfonic acid ($pK_a = -1.92$) and benzenesulfonic acid ($pK_a = -2.8$) [22]. Across the four computational methods, predicted values for methanesulfonic acid ranged from −1.39 to −3.15 (with an absolute deviation $|\Delta| = 0.5–1.2$ pK_a units relative to experiment), while benzenesulfonic acid was predicted between −1.83 and −3.88 ($|\Delta| \approx 1.0$ unit). The mean absolute deviation from experiments is approximately 0.8–1.1 pK_a units, which falls within the typical accuracy range reported for DFT-based pK_a calculations employing implicit solvation models. Importantly, all approaches reproduce the correct experimental ordering of acidity, with benzenesulfonic acid predicted to be more acidic

16163028, 2026, 69, Downloaded from https://advanced.onlinelibrary.wiley.com/doi/10.1002/adfm.77447, Wiley Online Library on [10/11/2026]. See the Terms and Conditions (https://onlinelibrary.wiley.com/terms-and-conditions) on Wiley Online Library for rules of use; OA articles are governed by the applicable Creative Commons License

TABLE 1 | Calculated pK_a values of sulfonic acid compounds from varied DFT methods/cycles.

Organic sulfonic acid	pK_a Cycle A		pK_a Cycle B		Fluorine-containing sulfonic acid	pK_a Cycle A		pK_a Cycle B	
	B3LYP	M06-2X	B3LYP	M06-2X		B3LYP	M06-2X	B3LYP	M06-2X
 **1**	−1.39	−2.03	−2.33	−3.15	 **2**	−10.60	−11.54	−11.58	−12.65
 **3**	−0.82	−1.69	−1.44	−2.81	 **4**	−10.56	−11.78	−11.53	−12.89
 **5**	−1.83	−2.77	−2.80	−3.88	 **6**	−6.08	−6.82	−7.05	−7.94
 **7**	−6.36	−7.32	−7.34	−8.44	 **8**	−10.21	−11.54	−11.18	−12.80

than methanesulfonic acid, indicating that the structural trends are robust with respect to methodological choice.

M06-2X systematically predicts lower pK_a values than B3LYP across the series for both thermodynamic cycles, typically by ~1 pK_a unit. This reflects the expected sensitivity of deprotonation free energies to the choice of exchange-correlation functional, although the relative ordering of acids is preserved with both functionals. When comparing calculation schemes, the water-assisted Cycle B generally predicts stronger acidity than Cycle A. This systematic shift (~0.9–1.2 pK_a unit) arises from differences in proton reference states and associated standard-state corrections [28] but does not alter qualitative trends across the series, indicating that both approaches are suitable for comparative analysis.

All calculated acids exhibited a significant decrease in pK_a upon fluorination. Alkylsulfonic acids showed a larger reduction in pK_a than arylsulfonic acids when fluorinated. Using the Cycle B/M06-2X protocol, trifluoromethanesulfonic acid (**2**, $pK_a = -12.65$) and perfluorohexanesulfonic acid (**4**, $pK_a = -12.89$), which are the fluorinated counterparts of methanesulfonic acid (**1**, $pK_a = -3.15$) and hexanesulfonic acid (**3**, $pK_a = -2.81$), respectively, showed a substantial decrease in their pKa values of approximately 9–10 units. This trend is attributed to the strong inductive effect of fluorinated alkyl chains, which withdraw electron density through σ bonds, stabilizing the conjugate base of sulfonic acids. In the case of aromatic sulfonic acid, the effect of fluorination on the ring was found to be weaker than that of fluorination on the alkyl chain, with a decrease of about 4 pK_a units (e.g., pentafluorobenzenesulfonic acid (**6**), $pK_a = -7.94$ and benzenesulfonic acid (**5**), $pK_a = -3.88$). The pentafluorophenyl group is inductively electron-withdrawing, but its effect is intermediate between that of a nearly neutral phenyl group and more strongly electron withdrawing trifluoromethyl group. This weaker inductive withdrawal relative to perfluoroalkyl substituents may result from disrupted p–π interactions between fluorine lone pairs and the aromatic π system, along with a minimal resonance electron-withdrawing contribution [29]. To further probe the influence of fluorine substitution and the competing roles of inductive and resonance effects on aromatic systems, *para*-substituted benzenesulfonic acids were examined (Table S1). *Para*-fluorination as in 4-fluorobenzenesulfonic acid (**9**, $pK_a = -3.37$) was found slightly less acidic relative to benzenesulfonic acid (**5**), whereas substitution with a trifluoromethyl group, as in 4-(trifluoromethyl)benzenesulfonic acid, resulted in significantly stronger acidity (**10**, $pK_a = -5.06$), reflecting the purely inductive electron-withdrawing character of the CF_3 group without compensating resonance effects. The pK_a value of the small molecule analogue of Nafion, perfluoro(2-ethoxyethane)sulfonic acid, was calculated to be −12.80 (**8**), comparable to that of perfluorohexanesulfonic acid (**4**, $pK_a = -12.89$). The result suggests that having a perfluoroether spacer attached to sulfonic acid does not diminish the through-bond inductive effect of a perfluoroalkyl chain.

The calculated acidity follows a clear hierarchy, with highly fluorinated and perfluorinated sulfonic acids exhibiting the strongest acidity, followed by α-fluorinated alkyl systems, substituted aromatic sulfonic acids, and finally non-fluorinated alkyl sulfonic acids. This trend highlights the dominant role of

16163028, 2026, 69, Downloaded from https://advanced.onlinelibrary.wiley.com/doi/10.1002/adfm.77447, Wiley Online Library on [10/11/2026]. See the Terms and Conditions (https://onlinelibrary.wiley.com/terms-and-conditions) on Wiley Online Library for rules of use; OA articles are governed by the applicable Creative Commons License

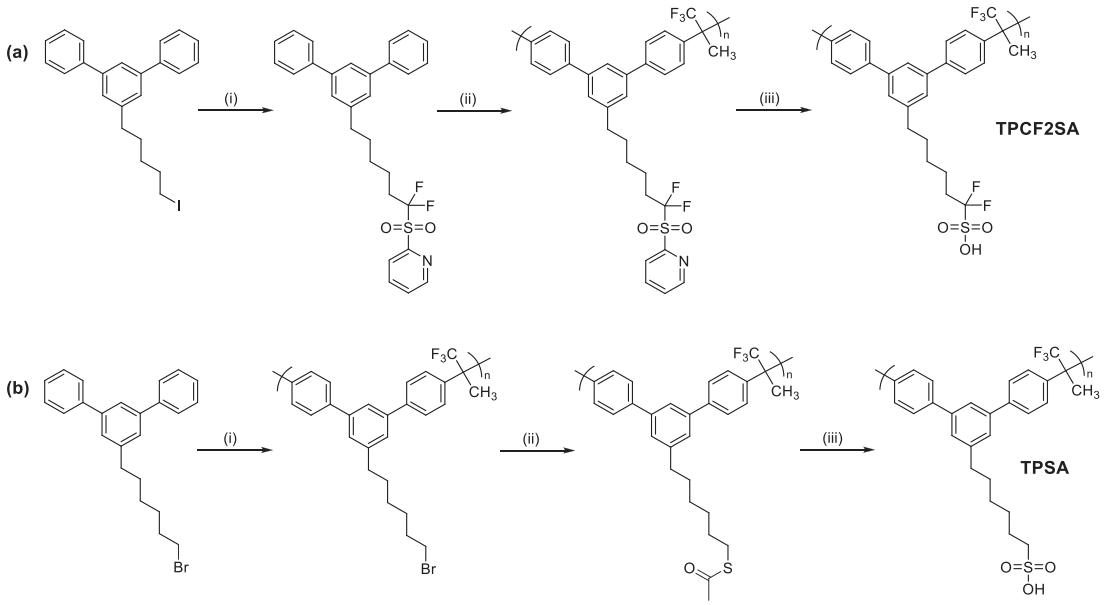


FIGURE 1 | The synthesis of hydrocarbon polymers with different acidity. (a) TPCF2SA: (i) 2-PySO_2CF_2H, LiHMDS, THF/HMPA, −98°C. (ii) CF_3COCH_3, CF_3SO_3H/CF_3COOH, CH_2Cl_2, 0°C. (iii) EtSNa, DMF/THF, rt.; 5% H_2O_2, rt. (b) TPSA: (i) CF_3COCH_3, CF_3SO_3H/CF_3COOH, CH_2Cl_2, 5°C. (ii) CH_3COSK, DMAc, 60°C. (iii) H_2O_2, CH_3COOH, H_2O/$(CH_3)_2CHOH$, 60°C.

inductive electron-withdrawing effects and their proximity to the sulfonic acid group. Although its effect is weaker than that of a perfluoroalkyl chain, fluorinating only the α-carbon adjacent to the sulfonic acid distinctly increases acidity. The calculated pK_a value of α,α-difluoro-1-hexanesulfonic acid (**7**) was pK_a = −8.44, compared with hexanesulfonic acid (**3**, pK_a = −2.81), corresponding to a decrease of more than 5 pK_a units. This result indicates that introducing a single CF_2 group at the α-carbon effectively provides a strong localized inductive effect, stabilizing the sulfonate conjugate base and yielding a significantly stronger acid compared to the corresponding non-fluorinated alkylsulfonic acid.

2.2 | Different Acidity Polymer Synthesis

We designed and synthesized two sulfonated hydrocarbon aromatic polymers with an identical backbone and membrane architecture, differing only in the proton donating strength of their side-chain sulfonic acid functionalities: one containing α,α-difluoro-1-hexanesulfonic acid groups and the other containing hexanesulfonic acid groups. We chose *m*-terphenyl as the aromatic backbone for its high molecular weight growth and strong chemical stability [30, 31], along with its favorable morphology and broad tunability through modular functionalization [32, 33]. This controlled design of proton exchange membranes allows a direct, comparative analysis of acidity-driven properties and performance differences. The synthetic route to these polymers is shown in Figure 1.

We introduced an alkyl α,α-difluorosulfonic acid moiety via nucleophilic difluoro(sulfonate)methylation to prepare the polymer, TPCF2SA (Figure 1a). In this method, reaction of the pentyl iodide-functionalized *m*-terphenyl via nucleophilic substitution with 2-((difluoromethyl)sulfonyl)pyridine yielded the pyridine-protected sulfonate precursor. The successful incorporation of difluorosulfonylpyridine was confirmed by ^{1}H and ^{19}F Nuclear magnetic resonance (NMR) spectroscopy (Figure S1) [34]. This reaction proceeded only with the alkyl iodide, and the corresponding alkyl bromo-functionalized *m*-terphenyl did not give the desired products, indicating insufficient reactivity of the alkyl bromide in this sensitive substitution. The monomer was sequentially polymerized with a stoichiometric amount of trifluoroacetone by acid-catalysed polyhydroalkylation [30], yielding a high molecular weight polymer, TPCF2Py, within 1 h (M_w 202.1 kg mol^{-1}, dispersity 3.3). The 2-pyridyl group remained intact (8.80, 8.10, 7.96, and partial 7.61–7.56 ppm, Figure 2a), effectively protecting the difluorosulfone functionality during polymerization. Finally, cleavage of the pyridyl group with sodium ethanethiolate, a mild basic nucleophile [34], generated difluoroalkylsulfonate and afforded the highly acidic hydrocarbon polymer TPCF2SA. Quantitative conversion was confirmed by ^{1}H NMR, where the pyridine peaks disappeared, and by ^{19}F NMR, where the difluoromethylene peak was shifted from −102.1 to −106.7 ppm (Figure 2b). Comparison of Fourier Transform Infrared (FTIR) spectra further confirmed the structure of the sulfonated polymer (Figure S2a). The SO_2 asymmetric stretch of the sulfonylpyridyl group at 1345 cm^{-1} shifted into the SO_3 asymmetric stretching region at 1213 cm^{-1} with the appearance of a broad O—H stretch at 3470 cm^{-1}.

The alkylsulfonic acid-containing counterpart polymer, TPSA, was synthesized to be compared with TPCF2SA (Figure 1b). The bromohexyl-substituted terphenyl monomer and trifluoroacetone were polymerized via acid-catalysed polyhydroalkylation [30]. The molecular weight of the polymer was M_w 412.9 kg mol^{-1} with dispersity of 3.5, higher than those of TPCF2Py, which may indicate more efficient molecular weight growth when using less bulky monomer. The alkyl bromo group then reacted with potassium thioacetate [35], resulting in a quantitative conversion into the precursor of sulfonic acid, confirmed by replacement of the CH_2Br peak at 3.36 ppm with thioacetate peaks at

16163028, 2026, 69, Downloaded from https://advanced.onlinelibrary.wiley.com/doi/10.1002/adfm.77447, Wiley Online Library on [10/11/2026]. See the Terms and Conditions (https://onlinelibrary.wiley.com/terms-and-conditions) on Wiley Online Library for rules of use; OA articles are governed by the applicable Creative Commons License

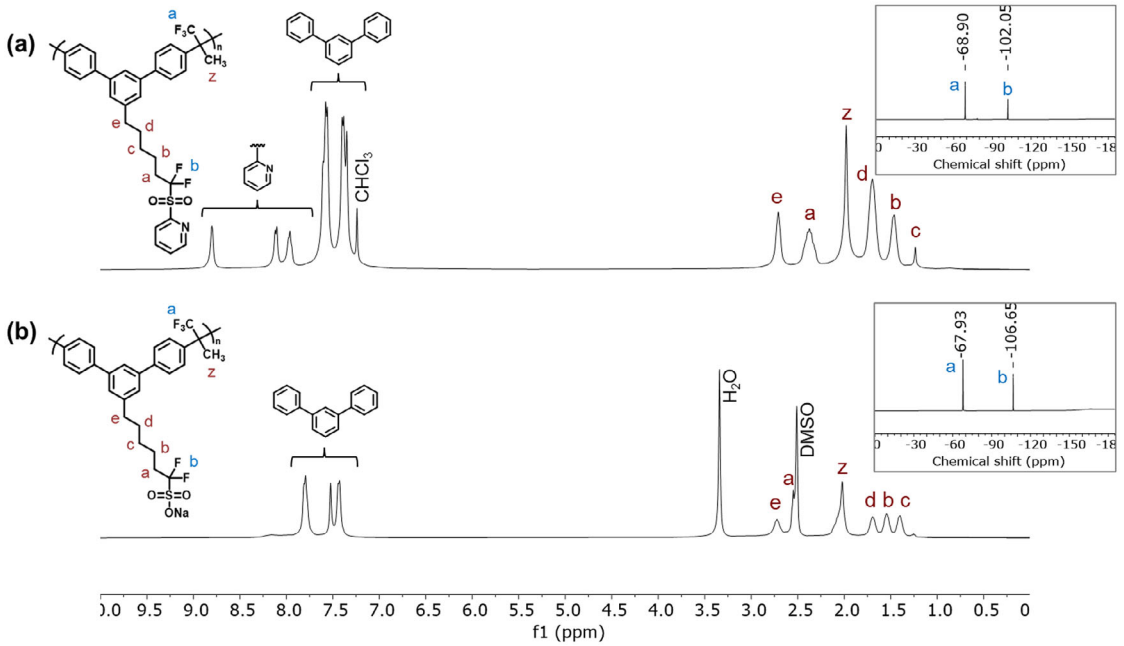


FIGURE 2 | NMR spectra of the highly acidic sulfonated polymer, TPCF2SA. (a) ^{1}H NMR of the precursor polymer TPCF2Py in $CDCl_3$ (inset: its ^{19}F NMR spectrum). (b) ^{1}H NMR of TPCF2SA after pyridyl deprotection in DMSO-d_6 (inset: its ^{19}F NMR spectrum).

TABLE 2 | Membrane properties.

Membrane	IEC (mequiv. g^{-1})[a]	Thickness (dry/wet, μm)	Water uptake (25/80°C, %)[b]	Swelling degree (25/80°C, %)[b]	λ (25/80°C)	H^+ σ (25/80°C, mS cm^{-1})[c]
TPCF2SA	1.8	60/65	8.8/20	7.8/14	2.7/6.2	40/87
TPSA	1.9	65/80	19/51	11/25	5.6/15	36/79
NR212	0.95	50/56	36/38	14/21	20/21	77/145

[a]The experimental IEC values determined by acid-base titration.
[b]The measurement was performed on membranes (H^+ form) after 24 h immersion in water.
[c]Measured in liquid water.

2.83 and 2.26 ppm in ^{1}H NMR spectra (Figure S3). The polymer was cast as a thin film and treated with hydrogen peroxide and acetic acid to convert thioacetate to sulfonic acid, forming an alkylsulfonic acid-functionalized proton exchange membrane. The chemical structure was verified by ^{1}H NMR spectra, which showed disappearance of the thioacetate peaks and appearance of CH_2SO_3H at 2.53 ppm in DMSO-d_6 (Figure S4b), and by FTIR which showed disappearance of the thioacetate C═O stretch at 1688 cm^{-1} along with the appearance of SO_3 bands at 1142 and 1037 cm^{-1} and a broad O—H stretch at 3385 cm^{-1} (Figure S2b).

2.3 | Characterization of Polymer Properties

The two sulfonated polymers, TPCF2SA and TPSA, were solvent cast into thin film membranes with thicknesses in the range of 60–65 μm. Both polymers exhibit good solubility in polar aprotic solvents and alcohols, while remaining insoluble in water (Table S2). Their physicochemical and transport properties were systematically evaluated and benchmarked against a commercial NR212 membrane, with results summarized in Table 2.

Both membranes showed good agreement between titrated IEC and the theoretical IEC calculated from NMR. TPSA exhibited a titrated IEC of 1.90 mequiv. g^{-1} vs. a theoretical value of 2.05 mequiv. g^{-1}, while TPCF2SA showed 1.78 mequiv. g^{-1} vs. 1.90 mequiv. g^{-1}. The slightly lower IEC of TPCF2SA is consistent with incorporation of the CF_2 group. These results indicate that the sulfonic acid contents are broadly consistent with the targeted polymer compositions. The small differences between theoretical and experimental IEC values, approximately 6%–7%, are likely due to inherent titration limitations, including incomplete ion exchange during sample preparation and endpoint uncertainty.

The thermal stability of the membranes was analyzed by thermogravimetric analysis (TGA) under nitrogen atmosphere (Figure S4). The thermogram showed that TPSA began to decompose at $T_{d,95}$ = 248°C, corresponding to the onset of desulfonation [36]. In contrast, TPCF2SA membrane did not reach $T_{d,95}$ until

16163028, 2026, 69, Downloaded from https://advanced.onlinelibrary.wiley.com/doi/10.1002/adfm.77447, Wiley Online Library on [10/11/2026]. See the Terms and Conditions (https://onlinelibrary.wiley.com/terms-and-conditions) on Wiley Online Library for rules of use; OA articles are governed by the applicable Creative Commons License

346°C, indicating that the difluorosulfonic acid group is thermally more stable than the alkylsulfonic acid group. In both cases, the membranes exhibited thermal stability far above the normal operating temperatures of most electrochemical devices.

Water uptake and dimensional swelling in liquid water were measured at 25°C and 80°C, revealing temperature-dependent differences in hydration behavior between the two hydrocarbon membranes under PEMWE-relevant conditions. TPCF2SA absorbed 8.8% and 20% of its dry weight at 25°C and 80°C, respectively, whereas TPSA exhibited markedly higher water uptake of 19% and 51% under the same condition. The same trend was observed in the swelling degree based on diagonal length change after immersion in liquid water. TPCF2SA exhibited swelling of 7.8% and 14% at 25°C and 80°C, respectively, while TPSA swelled by 11% and 25% under the same conditions. The lower water uptake and smaller dimensional change of TPCF2SA are favorable as they can help mitigate membrane deformation under hot, fully hydrated conditions. By contrast, the larger swelling of TPSA could be less desirable for device operation, although its dimensional change is still moderate compared with that of many reported hydrocarbon membranes [37].

These differences in water uptake are reflected in the hydration number, λ, which provides a more direct measure of the amount of water associated with each acid site. TPCF2SA exhibits notably low λ values of 2.7 and 6.2 at 25 and 80°C, respectively, whereas TPSA showed higher λ values of 5.6 and 15 under the same conditions. NR212 displayed higher λ values of 20 and 21, consistent with the well-known ability of PFSA membranes to retain substantial amounts of water within phase-separated ionic domains. Despite its comparatively low hydration number, TPCF2SA maintained high proton conductivity, reaching 40 and 87 mS cm^{-1} at 25°C and 80°C, respectively, compared with 36 and 79 mS cm^{-1} for TPSA. This is significant because many reported hydrocarbon PEMs achieve high conductivity only at higher hydration levels. For example, Pemion has been reported to exhibit water uptake of 225% and $\lambda \approx 40$ at 80°C, while even after crosslinking it remains at 120% and $\lambda \approx 24$ [20]. Likewise, sulfonated partially fluorinated poly(arylene ether)s with IEC near 3 mequiv. g^{-1} require 74%–143% water uptake at 80°C to reach conductivities above 0.17 S cm^{-1} [37]. Thus, TPCF2SA is notable not for its absolute conductivity alone, but for maintaining comparatively high proton conductivity at exceptionally low hydration and low swelling. In this regard, TPCF2SA demonstrates a unique combination of low water uptake and high conductivity that distinguish it from previously reported hydrocarbon PEMs.

Small angle x-ray scattering (SAXS) results suggest that the higher acidity of TPCF2SA helps it build a more effective proton-transport morphology, consistent with the conductivity and hydration trends described above. SAXS measurements in liquid water reveal clear differences in the nanostructure of the two hydrocarbon membranes that emerge at elevated temperature (Figure 3). At 25°C, both TPSA and TPCF2SA show relatively broad, diffuse scattering profiles without a sharply defined feature, indicating limited long-range structural correlation in the hydrated state. TPSA exhibits moderately higher overall scattering intensity than TPCF2SA, particularly at lower q, suggesting stronger large-scale scattering contrast or concentration fluctuations. Upon heating to 80°C, both membranes show increased low-q scattering, in agreement with enhanced structural heterogeneity under more highly hydrated conditions. A more pronounced change was observed for TPCF2SA at 80°C, where a distinct low-q scattering maximum corresponding to an apparent length scale of approximately 30 nm in the hydrated morphology. In contrast, TPSA at 80°C remains comparatively broad with no similarly distinct scattering maximum. These results suggest that TPCF2SA maintains a more distinguishable hydrated morphology under elevated-temperature aqueous conditions, likely due to its lower water uptake and reduced dimensional swelling relative to TPSA. This preserved hydrated morphological correlation may contribute to the favorable proton transport behavior of TPCF2SA under PEMWE-relevant conditions. When considered together with its lower λ and higher conductivity, this behavior is consistent and particularly significant because TPCF2SA achieves a phase-separated nanoscale morphology without the higher hydration observed for TPSA. This more favorable morphological organization likely arises in part from the stronger acidity of the CF_2-substituted sulfonic acid group, which promotes ionic segregation and local domain formation. The resulting ionic domain structure, together with enhanced proton dissociation, contributes to more efficient proton transport and the higher conductivity of TPCF2SA at lower water content.

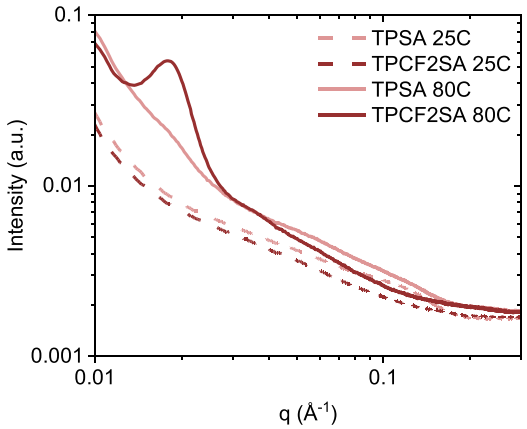


FIGURE 3 | Integrated SAXS profiles of the membranes in water at 25°C and 80°C. The TPCF2SA membrane shows a strong phase-separation at higher temperatures with a sharp, low-q peak corresponding to 32±2 nm of domain spacing.

2.4 | Water Electrolyzer Performance

For electrochemical characterization, membrane electrode assemblies (MEAs) were fabricated using catalyst coated membranes (CCMs) with an active area of 5 cm^2. IrO_x was used as the anode catalyst (0.4 mg cm^{-2}), Pt/C was used as the cathode catalyst (0.1 mg cm^{-2}), and Nafion D2020 served as the ionomer in both the catalyst layers. Single cell PEM water electrolyzer testing was performed at 80°C with water supplied only to the anode at a flow rate of 15 mL min^{-1}. For a straightforward initial comparison of membrane performance, all CCM preparation procedures and testing parameters were kept identical and followed the Nafion-optimized protocol. Note that the membrane thickness varies slightly across samples (Table 2), but the values fall within a comparable range (dry

16163028, 2026, 69, Downloaded from https://advanced.onlinelibrary.wiley.com/doi/10.1002/adfm.77447, Wiley Online Library on [10/11/2026]. See the Terms and Conditions (https://onlinelibrary.wiley.com/terms-and-conditions) on Wiley Online Library for rules of use; OA articles are governed by the applicable Creative Commons License

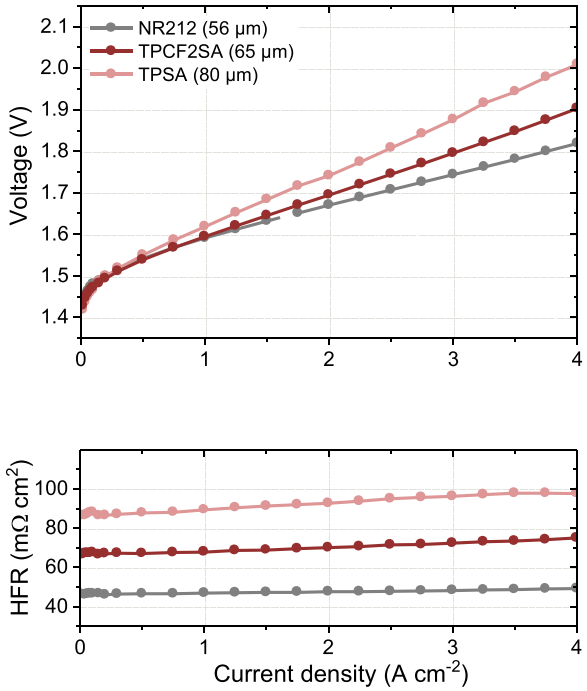


FIGURE 4 | Water electrolyzer performance comparison of TPCF2SA, TPSA, and NR212 as a baseline membrane. Anode: 0.40 mg_{Ir} cm^{-2}, cathode: 0.10 mg_{Pt} cm^{-2}. Ionomer: D2020. Temperature at 80°C, anode/cathode pressure = 1 atm, water flow rate = 15 mL min^{-1}.

thickness 50–65 μm, wet thickness 56–80 μm due to different water uptake and swelling of membranes).

Polarization curves (Figure 4) shows clear performance differences between the two hydrocarbon membranes (TPCF2SA and TPSA) with NR212 included as a benchmark. In the low-current region at 0.2 A cm^{-2}, the TPSA- and TPCF2SA-based MEAs operated at 1.42 and 1.43 V, respectively, both comparable to NR212 (1.43 V), indicating that these hydrocarbon membranes support similarly favorable electrode kinetics. The TPCF2SA MEA showed strong high-current performance, delivering 3.0 A cm^{-2} at 1.79 V, approaching the performance of NR212, which achieved 3.0 A cm^{-2} at 1.74 V. In contrast, TPSA required 1.88 V to reach 3.0 A cm^{-2} and delivered only 2.50 A cm^{-2} at 1.80 V. Overall, these results demonstrate that the hydrocarbon membrane with higher acidity, TPCF2SA supports significantly improved PEMWE performance relative to TPSA at elevated current densities while operating at comparatively low cell voltages. Notably, TPCF2SA performs comparably to NR212 despite its greater wet thickness (65 μm vs. 56 μm of NR212).

The observed polarization trends at high current density closely follow the high-frequency resistance (HFR) (Figure 4). TPSA exhibits the highest HFR, consistent with lower ionic conduction of alkylsulfonic acid and higher thickness (80 μm), both of which contribute to increased ohmic losses and higher operating voltages, especially at high current densities. NR212 shows the lowest HFR, reflecting its high proton conductivity and low thickness (56 μm). Despite its greater wet thickness than NR212 and its correspondingly higher HFR, TPCF2SA still achieves comparable overall voltage performance. This result indicates that the MEA based on TPCF2SA maintains strong electrolyzer performance despite a substantially larger ohmic penalty, highlighting the promise of this membrane chemistry beyond what would be expected from thickness or ex situ conductivity. Consistent with this interpretation, HFR-free polarization curves (Figure S5) shows the advantage of TPCF2SA, indicating its high performance is due to reduced non-ohmic contributions, while TPSA also shows improved performance in the kinetic-dominated regime.

The electrochemical impedance spectroscopy plots collected at 1.45 V further support these observations (Figure S6). The high-frequency intercepts follow the same order as the HFR values, with NR212 showing the lowest ohmic resistance, followed by TPCF2SA and TPSA. Differences in the impedance spectra further suggest variations in kinetic and/or interfacial contributions, with TPCF2SA appearing to show lower polarization resistance than TPSA and NR212, and NR212 showing the highest overall polarization resistance consistent with the observed HFR-free polarization curves (Figure S5). These results imply that, despite its lower ohmic resistance, NR212 may experience larger charge-transfer and/or interfacial transport losses at 1.45 V, although additional analysis would be needed in future studies to independently distinguish these contributions.

3 | Conclusion

In this work, we show that engineering the intrinsic acidity of sulfonic acid groups through α-CF_2 substitution provides a viable strategy to decouple proton conductivity from water uptake in hydrocarbon PEMs. The resulting membrane maintains high proton conductivity (87 mS cm^{-1} at 80°C) at a relatively low hydration number ($\lambda \approx 6$), significantly lower than typically observed for hydrocarbon and PFSA-based systems, while also exhibiting reduced water uptake and improved dimensional stability. These results indicate that increasing acid strength enables efficient proton dissociation and transport under limited hydration, reducing reliance on bulk water to sustain conductivity. These experimental observations are corroborated by DFT calculations, which show that α-CF_2 substitution effectively lowers the pK_a relative to corresponding alkylsulfonic acid analogue. Comparative analysis with the alkylsulfonic acid-containing PEM highlights that this improvement is not driven by IEC, but rather by enhanced proton transport efficiency per acid site and per water molecule. The ability to achieve high conductivity at low hydration suggests a shift toward acid-controlled transport, where enhanced intrinsic acidity supports efficient proton transport at lower hydration without requiring extensive water-mediated connectivity. This behavior contrasts with conventional hydrocarbon membranes, which typically require high hydration to form continuous proton-conducting pathways.

At the device level, the α-CF_2-functionalized membrane delivers competitive PEM water electrolyzer performance relative to NR212, despite lower water uptake and comparable membrane thickness, demonstrating that improved intrinsic transport properties can offset conventional limitations associated with hydrocarbon systems. However, long-term PEMWE durability testing remains an important direction for future work. These findings establish acidity engineering as an effective molecular design strategy for overcoming the long-standing tradeoff

16163028, 2026, 69, Downloaded from https://advanced.onlinelibrary.wiley.com/doi/10.1002/adfm.77447, Wiley Online Library on [10/11/2026]. See the Terms and Conditions (https://onlinelibrary.wiley.com/terms-and-conditions) on Wiley Online Library for rules of use; OA articles are governed by the applicable Creative Commons License

between proton conductivity and water uptake in hydrocarbon PEMs, enabling high electrolyzer performance without relying on excessive membrane hydration.

Acknowledgements

This work was supported by the U.S. Department of Energy through the Los Alamos National Laboratory. Los Alamos National Laboratory is operated by Triad National Security, LLC, for the National Nuclear Security Administration of U.S. Department of Energy (Contract No. 89233218CNA000001). Research presented in this work was supported by the Laboratory Directed Research and Development program of Los Alamos National Laboratory under project 20240061DR. A Kusoglu and DIK would like to acknowledge the Alternative Fuels and Feedstocks Office (previously Hydrogen and Fuel Cell Technologies Program) of the Critical Materials and Energy Innovation Office of the U.S. Department of Energy, under contract number DE-AC02–05CH11231. This paper made use of beamline 7.3.3. at the Advanced Light Source (ALS), supported by the Office of Science, Office of Basic Energy Sciences, of the U.S. DOE (Contract No. DE-AC02-05CH11231).

Funding

This work was financially supported by the Laboratory Directed Research and Development program of Los Alamos National Laboratory under project 20240061DR and Hydrogen and Fuel Cell Technologies Program in the Critical Materials and Energy Innovation Office of the U.S. Department of Energy (No. DE-AC02-05CH11231).

Conflicts of Interest

The authors declare no conflicts of interest.

Data Availability Statement

The data that support the findings of this study are available in the supplementary material of this article.

References

1. K. D. Kreuer, "On the Development Of Proton Conducting Polymer Membranes For Hydrogen And Methanol Fuel Cells," *Journal of Membrane Science* 185 (2001): 29.

2. A. Kusoglu and A. Z. Weber, "New Insights Into Perfluorinated Sulfonic-Acid Ionomers," *Chemical Reviews* 117 (2017): 987.

3. G. M. Su, I. A. Cordova, M. A. Yandrasits, et al., "Chemical and Morphological Origins Of Improved Ion Conductivity In Perfluoro Ionene Chain Extended Ionomers," *Journal of the American Chemical Society* 141 (2019): 13547.

4. M. H. Dehghani, M. Aghaei, P. Bashardoust, et al., "An Insight Into The Environmental And Human Health Impacts Of Per-And Polyfluoroalkyl Substances (Pfas): Exploring Exposure Pathways And Their Implications," *Environmental Sciences Europe* 37 (2025): 81.

5. C. H. Fujimoto, M. A. Hickner, C. J. Cornelius, and D. A. Loy, "Ionomeric poly (phenylene) prepared by Diels– Alder Polymerization: Synthesis And Physical Properties Of A Novel Polyelectrolyte," *Macromolecules* 38 (2005): 5010.

6. J. Miyake and K. Miyatake, "Fluorine-Free Sulfonated Aromatic Polymers As Proton Exchange Membranes," *Polymer Journal* 49 (2017): 487.

7. L. Zarybnicka and E. Stranska, "Study of Effect Of Two Sulfonating Agents On Electrochemical Properties Of Surface-Modified Polyethersulfone Membrane," *Journal of Applied Polymer Science* 137 (2020): 48826.

8. C. M. Leo, S. N. Alonzo, E. Grumbles, and J. G. Kennemur, "Sulfonated Aromatic Polypentenamers: Scope Of The Acetyl Sulfate Reaction," *Macromolecules* 57 (2024): 8610.

9. T. J. G. Skalski, B. Britton, T. J. Peckham, and S. Holdcroft, "Structurally-Defined, Sulfo-Phenylated, Oligophenylenes And Polyphenylenes," *Journal of the American Chemical Society* 137 (2015): 12223.

10. W. L. Harrison, F. Wang, J. B. Mecham, et al., "Influence of the Bisphenol Structure On The Direct Synthesis Of Sulfonated Poly (Arylene Ether) Copolymers. I," *Journal of Polymer Science Part A: Polymer Chemistry* 41 (2003): 2264.

11. J. Miyake, R. Taki, T. Mochizuki, et al., "Design of Flexible Polyphenylene Proton-Conducting Membrane For Next-Generation Fuel Cells," *Science Advances* 3 (2017): aao0476.

12. F. Pierre, B. Commarieu, A. C. Tavares, and J. Claverie, "High Tg Sulfonated Insertion Polynorbornene Ionomers Prepared By Catalytic Insertion Polymerization," *Polymer* 86 (2016): 91.

13. N. R. Kang, T. H. Pham, and P. Jannasch, "Polyaromatic Perfluorophenylsulfonic Acids With High Radical Resistance And Proton Conductivity," *ACS Macro Letters* 8 (2019): 1247.

14. H. Nguyen, F. Lombeck, C. Schwarz, et al., "Hydrocarbon-based Pemion™ Proton Exchange Membrane Fuel Cells With State-Of-The-Art Performance," *Sustainable Energy & Fuels* 5 (2021): 3687.

15. F. O. Egemole, A. L. G. Biancolli, and S. Holdcroft, "Water Electrolysis Using Fluorine-Free, Reinforced Sulfo-Phenylated Polyphenylene Membranes," *Electrochimica Acta* 508 (2024): 145259.

16. K. A. Weber, C. S. Harzer, E. Bindl, K. Stengl, and H. A. Gasteiger, "Editors' Choice—Can Hydrocarbon-Based MEAs Close the Performance Gap to State-of-the-Art Perfluorosulfonic Acid-Based MEAs for PEM Fuel Cells?," *ECS Advances* 4 (2025): 034501.

17. T. J. G. Skalski, M. Adamski, B. Britton, et al., "Sulfophenylated Terphenylene Copolymer Membranes And Ionomers," *Chemsuschem* 11 (2018): 4033.

18. S. J. Hong, H. Y. Jung, S. J. Yoon, et al., "Constrained Hydrocarbon-Based Ionomers In Porous Poly (tetrafluoroethylene) Supports For Enhanced Durability Of Polymer Electrolyte Membrane Fuel Cells And Water Electrolyzers," *Journal of Power Sources* 551 (2022): 232221.

19. A. Zucconi, J. Hack, R. Stocker, T. A. M. Suter, A. J. E. Rettie, and D. J. L. Brett, "Challenges and Opportunities For Characterisation Of High-Temperature Polymer Electrolyte Membrane Fuel Cells: A Review," *Journal of Materials Chemistry A* 12 (2024): 8014.

20. C. Schare, G. Titvinidze, N. Platenburg, et al., "Crosslinked Sulfonated Polyphenylenes: Overcoming The Performance–Gas Permeation–Stability Trilemma In Water Electrolyzers," *Journal of Materials Chemistry A* 13 (2025): 19292.

21. Y. Chang, A. D. Mohanty, S. B. Smedley, et al., "Effect of Superacidic Side Chain Structures On High Conductivity Aromatic Polymer Fuel Cell Membranes," *Macromolecules* 48 (2015): 7117.

22. J. P. Guthrie, "Hydrolysis of Esters Of Oxy Acids: P K a Values For Strong Acids; Brønsted Relationship For Attack Of Water At Methyl; Free Energies Of Hydrolysis Of Esters Of Oxy Acids; And A Linear Relationship Between Free Energy Of Hydrolysis And p K a Holding Over A Range Of 20 p K Units," *Canadian Journal of Chemistry* 56 (1978): 2342.

23. A. Kütt, S. Selberg, I. Kaljurand, et al., "pKa Values In Organic Chemistry–Making Maximum Use Of The Available Data," *Tetrahedron Letters* 59 (2018): 3738.

24. F. R. Dutra, C. S. Silva, and R. Custodio, "On the Accuracy of the Direct Method to Calculate pKa from Electronic Structure Calculations," *The Journal of Physical Chemistry A* 125 (2021): 65.

25. G. C. Shields and P. G. Seybold, *Computational Approaches for the Prediction of pKa Values CRC Press* (Boca Raton, 2013).

26. M. D. Tissandier, K. A. Cowen, W. Y. Feng, et al., "The proton's absolute aqueous enthalpy and Gibbs free Energy Of Solvation From

16163028, 2026, 69, Downloaded from https://advanced.onlinelibrary.wiley.com/doi/10.1002/adfm.77447, Wiley Online Library on [10/11/2026]. See the Terms and Conditions (https://onlinelibrary.wiley.com/terms-and-conditions) on Wiley Online Library for rules of use; OA articles are governed by the applicable Creative Commons License

Cluster-Ion Solvation Data," *The Journal of Physical Chemistry A* 102 (1998): 7787.

27. J. R. Pliego Jr and J. M. Riveros, "Gibbs Energy Of Solvation Of Organic Ions In Aqueous And Dimethyl Sulfoxide Solutions," *Physical Chemistry Chemical Physics* 4 (2002): 1622.

28. J. Ho and M. L. Coote, "A Universal Approach For Continuum Solvent pKa Calculations: Are We There Yet?," *Theoretical Chemistry Accounts* 125 (2010): 3.

29. W. A. Sheppard, "Pentafluorophenyl group. Electronic Effect As A Substituent," *Journal of the American Chemical Society* 92 (1970): 5419.

30. W.-H. Lee, E. J. Park, J. Han, D. W. Shin, Y. S. Kim, and C. Bae, "Poly (terphenylene) Anion Exchange Membranes: The Effect Of Backbone Structure On Morphology And Membrane Property," *ACS Macro Letters* 6 (2017): 566.

31. E. J. Park, C. B. Capuano, K. E. Ayers, and C. Bae, "Chemically Durable Polymer Electrolytes For Solid-State Alkaline Water Electrolysis," *Journal of Power Sources* 375 (2018): 367.

32. B. Xue, R.-B. Zang, J.-R. Wu, et al., "Positional Engineering of Ionic Side Chains Enhances π-π Stacking in Poly (m-Terphenylene Alkylene) Anion Exchange Membranes to Address the Conductivity-Stability Tradeoff," *Macromolecules* 58 (2025): 11302.

33. T. H. Pham, J. S. Olsson, and P. Jannasch, "Effects of the N -Alicyclic Cation And Backbone Structures On The Performance Of Poly(Terphenyl)-Based Hydroxide Exchange Membranes," *Journal of Materials Chemistry A* 7 (2019): 15895–15906, https://doi.org/10.1039/C9TA05531B.

34. G. S. Prakash, C. Ni, F. Wang, J. Hu, and G. A. Olah, "From Difluoromethyl 2-Pyridyl Sulfone to Difluorinated Sulfonates: A Protocol for Nucleophilic Difluoro(sulfonato)methylation," *Angewandte Chemie International Edition* 50 (2011): 2559–2563, https://doi.org/10.1002/anie.201007594.

35. M. K. Pagels, S. Adhikari, R. C. Walgama, et al., "One-Pot Synthesis of Proton Exchange Membranes From Anion Exchange Membrane Precursors," *ACS Macro Letters* 9 (2020): 1489–1493, https://doi.org/10.1021/acsmacrolett.0c00550.

36. A. Buonerba, V. Speranza, and A. Grassi, "Novel Synthetic Strategy For The Sulfonation Of Polybutadiene And Styrene–Butadiene Copolymers," *Macromolecules* 46 (2013): 778.

37. W. Li, R. Zhang, X. Zhao, Z. Yue, H. Qian, and H. Yang, "Highly Proton Conductive And Stable Sulfonated poly(arylene-alkane) for FUEL CELLS WITH PERFORmance Over 2.46 W cm^{-2}," *Journal of Materials Chemistry A* 11 (2023): 4547–4558, https://doi.org/10.1039/D2TA08911D.

Supporting Information

Additional supporting information can be found online in the Supporting Information section.

Supporting File: adfm77447-sup-0001-SuppMat.docx.

16163028, 2026, 69, Downloaded from https://advanced.onlinelibrary.wiley.com/doi/10.1002/adfm.77447, Wiley Online Library on [10/11/2026]. See the Terms and Conditions (https://onlinelibrary.wiley.com/terms-and-conditions) on Wiley Online Library for rules of use; OA articles are governed by the applicable Creative Commons License